Comparative Biochemistry and Physiology, Part A 270 (2022) 111232

Contents lists available at ScienceDirect

Comparative Biochemistry and Physiology, Part A

journal homepage: www.elsevier.com/locate/cbpa

Metabolic and molecular evidence for long-chain PUFA biosynthesis capacity in the grass carp *Ctenopharyngodon idella*

Manuel Marrero [a,*], Óscar Monroig [b], Juan Carlos Navarro [b], Alberto Ribes-Navarro [b], José Antonio Pérez [a], Ana Galindo [a], Covadonga Rodríguez [a]

[a] Departamento de Biología Animal, Edafología y Geología, Universidad de La Laguna, La Laguna 38206, Santa Cruz de Tenerife, Spain
[b] Instituto de Acuicultura Torre de la Sal (IATS), CSIC, 12595 Ribera de Cabanes, Castellón, Spain

ARTICLE INFO

Edited by Michael Hedrick

Keywords:
DHA
EPA
Fatty acyl desaturases
Elongation of very long-chain fatty acid protein
Grass carp

ABSTRACT

There is a growing interest to understand the capacity of farmed fish species to biosynthesise the physiologically important long-chain ($\geq C_{20}$) n-3 and n-6 polyunsaturated fatty acids (LC-PUFAs), eicosapentaenoic acid (EPA), docosahexaenoic acid (DHA) and arachidonic acid (ARA), from their C_{18} PUFA precursors available in the diet. In fish, the LC-PUFA biosynthesis pathways involve sequential desaturation and elongation reactions from α-linolenic acid (ALA) and linoleic acid (LA), catalysed by fatty acyl desaturases (Fads) and elongation of very long-chain fatty acids (Elovl) proteins. Our current understanding of the grass carp (*Ctenopharyngodon idella*) LC-PUFA biosynthetic capacity is limited despite representing the most farmed finfish produced worldwide. To address this knowledge gap, this study first aimed at characterising molecularly and functionally three genes (*fads2*, *elovl5* and *elovl2*) with putative roles in LC-PUFA biosynthesis. Using an *in vitro* yeast-based system, we found that grass carp Fads2 possesses Δ8 and Δ5 desaturase activities, with Δ6 ability to desaturate not only the C_{18} PUFA precursors (ALA and LA) but also 24:5n-3 to 24:6n-3, a key intermediate to obtain DHA through the "Sprecher pathway". Additionally, the Elovl5 showed capacity to elongate C_{18} and C_{20} PUFA substrates, whereas Elovl2 was more active over C_{20} and C_{22}. Collectively, the molecular cloning and functional characterisation of *fads2*, *elovl5* and *elovl2* demonstrated that the grass carp has all the enzymatic activities required to obtain ARA, EPA and DHA from LA and ALA. Importantly, the hepatocytes incubated with radiolabelled fatty acids confirmed the yeast-based results and demonstrated that these enzymes are functionally active.

1. Introduction

Long-chain ($\geq C_{20}$) polyunsaturated fatty acids (LC-PUFAs) are essential nutrients involved in critical biological processes since they play key structural roles in cellular biomembranes, participating in signalling and gene expression processes (Tocher, 1995; Guillou et al., 2010). Specifically, the n-3 LC-PUFAs, namely eicosapentaenoic acid (EPA, 20:5n-3) and docosahexaenoic acid (DHA, 22:6n-3), have been found to present beneficial effects in several pathologies affecting human health (Lauritzen et al., 2001; Salem et al., 2001; Innes and Calder, 2018; Mallick et al., 2019).

Generally, biosynthesis of LC-PUFAs from their C_{18} PUFA precursors, linoleic acid (LA, 18:2n-6) and α-linolenic acid (ALA, 18:3n-3), is low in human adults where only a 5% of ALA is estimated to be converted into n-3 LC-PUFAs (Barceló-Coblijn and Murphy, 2009). Therefore, an adequate dietary provision of n-3 LC-PUFAs must be achieved to guarantee the above-mentioned health benefits.

Marine organisms are the most important source of n-3 LC-PUFAs for humans (Pereira et al., 2003; Gladyshev et al., 2013; Monroig and Kabeya, 2018). However, many fisheries are currently overexploited and aquaculture has been proposed as the prime candidate to meet the increasing global demand for fish and seafood (Hixson, 2014; FAO, 2020). Paradoxically, feed manufacturing for finfish aquaculture is highly dependent upon fish oil (FO) and fishmeal (FAO, 2020), resulting

Abbreviations: ALA, α-linolenic acid; ARA, arachidonic acid; aa, amino acid; CEIBA, Ethics and Animal Welfare Committee; cDNA, complementary DNA; DHA, docosahexaenoic acid; DPA, docosapentaenoic acid; EPA, eicosapentaenoic acid; Elovl, fatty acyl elongase; FAF-BSA, fatty acid-free bovine serum albumin; FAME, fatty acid methyl ester; Fads, fatty acyl desaturases; FO, fish oil; HBSS, Hanks Balanced Salt Solution; HPGG, heme-binding motif; LA, linoleic acid; LB, Luria–Bertani; ORF, open reading frame; TPA, tetracosapentaenoic acid; THA, tetracosahexaenoic acid; TL, total lipid; TSA, Transcriptomic Shotgun Assembly; VO, vegetable oil.

* Corresponding author.
E-mail address: mmarrera@ull.edu.es (M. Marrero).

https://doi.org/10.1016/j.cbpa.2022.111232
Received 7 March 2022; Received in revised form 9 May 2022; Accepted 10 May 2022
Available online 14 May 2022

in an unsustainable practice which limits its expansion. Therefore, FO has been progressively replaced by vegetable oils (VOs) devoid of LC-PUFA, potentially impacting fish health and decreasing its nutritional value for consumers (Rodríguez et al., 2002; Mourente and Bell, 2006; Turchini et al., 2009; Pérez et al., 2014). In this regard, there is increasing interest to understand the abilities and mechanisms involved in the biosynthetic pathways of LC-PUFA in farmed fish species in order to develop rearing strategies to ensure the efficient and effective inclusion of VOs in aquafeeds formulation.

The production of LC-PUFAs from their C_{18} PUFA precursors, involve the action of two rate-limiting enzyme types, namely fatty acyl desaturases (Fads) and elongation of very long-chain fatty acid (Elovl) proteins (Fig. 1) (Castro et al., 2016). Fads are often denoted as "Δx desaturases" whereby x indicates the position of the newly inserted unsaturation (double bond), counting from the carboxyl group of the fatty acyl chain (Castro et al., 2016). With some exceptions reported in early emerged teleosts such as eels (Lopes-Marques et al., 2018), the vast majority of teleosts possess *fads2* as the unique *fads*-like desaturase in their genomes. Interestingly, functions of teleost Fads2 have diversified and, along the most commonly Δ6/Δ8 pattern also present in non-teleost vertebrates (Castro et al., 2016), teleost Fads2 include desaturase enzymes with Δ4 and Δ5 capacities (Castro et al., 2016; Monroig et al., 2018; Galindo et al., 2021). Along desaturases, Elovl enzymes catalyse the condensation reaction in the fatty acid elongation pathway resulting in the addition of two carbon units at the carboxyl end of the pre-existing fatty acyl chain (Jakobsson et al., 2006). Elovl5 and Elovl2 are arguably the main elongases involved in the LC-PUFA biosynthetic pathways. In agreement with their common evolutionary origin (Monroig et al., 2016), both Elovl5 and Elovl2 have elongation capacity towards C_{18}-C_{22} PUFA substrates. While Elovl5 has higher affinity towards C_{18} PUFAs, Elovl2 is more efficient in the elongation of C_{22} PUFAs (Castro et al., 2016). Both Fads and Elovl enzymes operate in a coordinated manner to convert dietary essential LA and ALA into the physiologically important arachidonic acid (ARA, 20:4n-6), and EPA and DHA, respectively, *via* two different metabolic pathways. Briefly, the "Δ6 pathway" consists of a Δ6 desaturation of LA or ALA, followed by an elongation step and a Δ5 desaturation to ARA or EPA, respectively, while the alternative route ("Δ8 pathway") begins with an elongation of LA or ALA, followed by two consecutive desaturations steps (Δ8 and Δ5) towards ARA or EPA (Fig. 1). Similarly, DHA can be biosynthesised by two alternative routes. First, a more direct route termed the "Δ4 pathway" consisting of an elongation of EPA to docosapentaenoic acid (DPA, 22:5n-3) and a subsequent Δ4 desaturation to DHA. Second, the "Sprecher pathway", firstly discovered in rats (Sprecher et al., 1995) and later confirmed in fish (Buzzi et al., 1997; Rodríguez et al., 2002; Oboh et al., 2017), consists of two consecutive elongations from EPA to tetracosapentaenoic acid (TPA, 24:5n-3), followed by a Δ6 desaturation to tetracosahexaenoic acid (THA, 24:6n-3) and a final chain-shortening through partial β-oxidation in peroxisomes (Fig. 1).

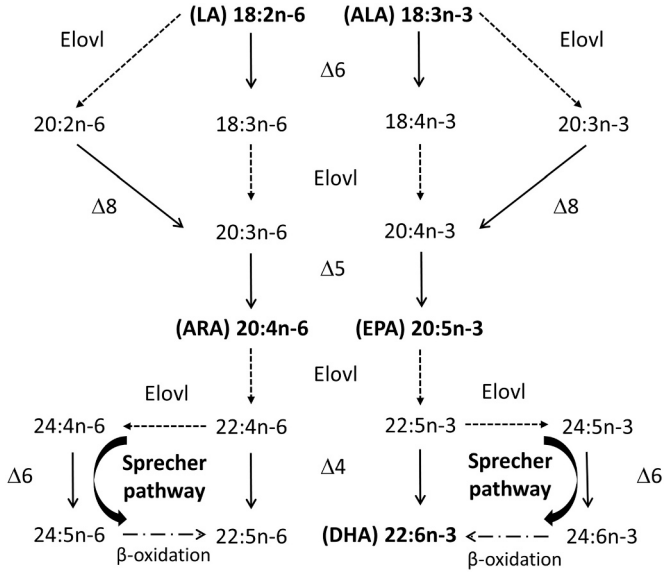

Fig. 1. Long-chain polyunsaturated fatty acid biosynthetic pathways from the C18 precursors linoleic acid (LA, 18:2n-6) and α-linolenic acid (ALA, 18:3n-3) in teleosts. Reactions catalysed by front-end desaturases ("Δx") are indicated with solid arrows. Elongation reactions are denoted as "Elovl" (dashed lines).

Historically, it had been widely accepted that freshwater and salmonid species had higher capacity for LC-PUFA biosynthesis than marine species (Tocher, 2010), accounted for the high evolutionary pressure to retain the ability to endogenously produce LC-PUFAs in an environment with low availability of these essential nutrients (Monroig et al., 2018; Ishikawa et al., 2019). Nowadays, this vision is regarded as too simplistic since other factors such as the trophic level and trophic ecology have been also suggested to influence the LC-PUFA production in teleosts (Castro et al., 2016). Moreover, the position of a certain species in the tree of life of bony fishes is crucial in determining the repertoire and, to some extent, the function of key Fads and Elovl enzymes involved in the LC-PUFA biosynthetic pathways, as well as on the mechanisms regulating their activity (Sarker et al., 2011; Fonseca-Madrigal et al., 2012; Galindo et al., 2021; Luo et al., 2021; Marrero et al., 2021; Xie et al., 2021). Otomorphans such as the amazonian tambaqui (*Colossoma macropomum*) and the african catfish (*Clarias gariepinus*) possess all required enzymes for the conversion of C18 PUFA to LC-PUFA (Oboh et al., 2016; Ferraz et al., 2019). Similarly, several cyprinids including the malaysian mahseer (*Tor tambroides*), tench (*Tinca tinca*), common carp (*Cyprinus carpio*) and zebrafish (*Danio rerio*) have a Fads2 with dual Δ6/Δ5 desaturase activities, besides the Elovl5 and Elovl2 required to biosynthesise LC-PUFA through the Sprecher pathway (Hastings et al., 2001; Zheng et al., 2004; Garrido et al., 2020; Sam et al., 2021). However, our current understanding on the LC-PUFA biosynthetic capacity of the grass carp *Ctenopharyngodon idella* remains rather limited, with only partial functional analyses being available for its *fads2* (Xie et al., 2020).

Importantly, the price of grass carp aquafeeds has increased over the last decade, raising the costs of production despite the improvements in its culture technology, while its market price has varied slightly (Xie et al., 2018). Incentive for culturing grass carp remains high because of market demand, and, in this sense, the understanding of mechanisms related with LC-PUFA biosynthesis are critical to improve feed formulations in order to decrease the production costs and maintain its meat quality.

This work aim to determine *C. idella* capacity to biosynthesise LC-PUFA through molecular cloning and functional characterisation of three genes (*fads2*, *elovl5* and *elovl2*) encoding the enzymes involved. We further investigated the actual enzymatic activity of the pathways by *in vitro* metabolism assays in hepatocytes incubated with [1-^{14}C] ALA, [1-^{14}C] LA and [1-^{14}C] EPA.

2. Materials and methods

This study was carried out in accordance with the Guidelines of the European Union Council (2010/63/EU) and the Spanish Government (RD1201/2005; RD53/2013 and law 32/2007) for the use of experimental animals for scientific purposes. The experiment was authorised by the Ethics and Animal Welfare Committee (CEIBA) of University of La Laguna (Spain).

2.1. Molecular cloning of fads2, elovl5 and elovl2 cDNAs

Adult *C. idella* was sacrificed with 0.02% (*v*/v) 2-phenoxyethanol, and ~ 100 mg of brain and liver collected. The tissue samples were immediately placed in tubes containing RNAlater (Qiagen Iberia S.L.,

Spain), and maintained at 4 °C for 24 h prior to be frozen at −20 °C until analysis. Total RNA was extracted from *C. idella* liver and brain using the Maxwell®16 instrument and the Maxwell® 16 LEV simplyRNA Purification Kit (Promega, Madison, WI, USA) following manufacturer's instructions. First strand complementary DNA (cDNA) was synthesised from 2 μg of RNA mix (brain and liver, 1:1) using Moloney Murine Leukemia Virus Reverse Transcriptase (M-MLV RT) (Promega) as indicated by manufacturer. To obtain full-length *fads2* and *elovl2* sequences *in silico*, *C. idella* partial *fads2* sequence (**AY445923.1**) and *D. rerio* complete *elovl2* sequence (**NM_001040362.1**) were used as queries to run BLAST searches for homologous sequences within the Transcriptomic Shotgun Assembly (TSA) database of *C. idella*; taxid: 7959 (accessed on 17 September 2019). Partial TSA sequences were subsequently assembled with the online tool cap3 (http://doua.prabi.fr/software/cap3). Gene specific primers designed in the 5'UTR (CI_fads2_U5F/CI_elovl2_U5F) and the 3'UTR (CI_fads2_U3R/CI_elovl2_U3R) of the assembled sequences were used to obtain a 1393 bp and 952 bp products by PCR (Phusion Green High-Fidelity DNA Polymerase) including the open reading frame (ORF) sequences of the putative *fads2* and *elovl2*, respectively. The corresponding PCR products were purified on a 1% (*w/v*) agarose gel using the Wizard® SV Gel and PCR Clean-Up System (Promega Biotech Ibérica SL, Madrid, Spain), and identified by DNA sequencing (DNA Sequencing Service, IBMCP-UPV, Valencia, Spain). Furthermore, the complete coding sequence of *elovl5* was obtained from GenBank (HQ637463.1). The ORF of the corresponding target genes were identified using the NCBI ORF Finder tool (www.ncbi.nlm.nih.gov/orffinder (accessed on 17 September 2019)), and then isolated by PCR using brain:liver cDNA as template, and primers with specific restriction sites for further cloning into pYES2 vector (Table 1). PCR products and pYES2 were subsequently digested with *Hin*d III and *Xho* I restriction enzymes (Promega) and ligated. The ligation reactions were transformed into the *Escherichia coli* competent TOP10™ strain (Invitrogen, Thermo Fisher Scientific, Madrid, Spain) and positive colonies were grown overnight in Luria–Bertani (LB) broth containing ampicillin (100 μg/mL). Sequences of inserts in each plasmid construct were confirmed by DNA sequencing (IBMCP-UPV) before being used to transform yeast competent cells.

2.2. Sequence and phylogenetic analysis of the C. idella Fads2, Elovl 5 and Elovl2

As described by Ribes-Navarro et al. (2021), the putative amino acid (aa) sequences of the Fads2, Elovl5 and Elovl2 from *C. idella* were predicted with ORF Finder tool (www.ncbi.nlm.nih.gov/orffinder/). The transmembrane regions of the *C. idella* Fads2, Elovl5 and Elovl2 were predicted using the topology prediction algorithm TMHMM online tool (www.cbs.dtu.dk/services/TMHMM/). A phylogenetic analysis comparing the aa sequences of Fads2, Elovl5 and Elovl2 from *C. idella* with other vertebrates, mostly teleost, was performed. The phylogenetic tree and all the corresponding analyses were performed using the CIPRES platform (Miller et al., 2010) (https://www.phylo.org/). Briefly, a MAFFT alignment and subsequent trimming (TrimAI) were performed followed by running a model test run in order to select the best evolutionary model for aa substitution. Finally, randomised accelerated maximum likelihood (RAxML) was conducted in order to build the phylogenetic tree. The best-fit evolutionary model was selected to JTT + I + G4 for the three genes by ModelTest-NG (Darriba et al., 2020). Confidence in the resulting phylogenetic tree branch topology was measured by bootstrapping through 1000 iterations, following the transfer distance bootstrap approach (Lemoine et al., 2018; Lutteropp et al., 2020).

2.3. Functional characterisation of the C. idella Fads2, Elovl5 and Elovl2 by heterologous expression in yeast

As described by Ferraz et al. (2019), the plasmid constructs pYES2-fads2, pYES2-elovl5 and pYES2-elovl2 were transformed into *Saccharomyces cerevisiae* competent cells (strain INVSc1) (Life Technologies). The empty vector pYES2 was used to transform a control yeast that confirmed no activity towards any of the tested substrates. One single recombinant colony from each transformation plasmid construct (pYES2-fads2, pYES2-elovl5 and pYES2-elovl2) and the pYES2-empty (control) were grown in SCMM^{-ura} broth for 2 d at 30 °C to produce a bulk culture with an OD600 of 8–10. Then, an appropriate volume of the yeast bulk cultures was inoculated in 5 mL of SCMM^{-ura} broth contained in individual 150 mL Erlenmeyer flasks to reach an OD600 of 0.4. The recombinant yeast in each Erlenmeyer flasks was grown for 4 h at 30 °C under constant shaking (250 rpm) until they reached an OD600 of ~1, at which point the transgene expression was induced by supplementing the culture media with galactose at 2% (*w/v*). To test the ability of the enzymes, transgenic yeast expressing the *C. idella fads2* were grown in the presence of a series of exogenously supplemented PUFA substrates to test the Δ6 (18:3n-3; 18:2n-6; 24:5n-3), Δ8 (20:3n-3; 20:2n-6), Δ5 (20:4n-3; 20:3n-6) and Δ4 (22:5n-3; 22:4n-6) desaturase capabilities. Additionally, yeast expressing the *C. idella elovl5* and *elovl2* were grown in the presence of different PUFA substrates to test the $C_{18} \rightarrow C_{20}$ (18:3n-3; 18:2n-6; 18:4n-3; 18:3n-6), $C_{20} \rightarrow C_{22}$ (20:5n-3; 20:4n-6) and $C_{22} \rightarrow C_{24}$ (22:5n-3; 22:4n-6) elongase activities. After 48 h of incubation, yeast was harvested by centrifugation and washed twice in double distilled water prior being preserved at −20 °C for further fatty acid analysis.

2.4. Fatty acid analysis

Total lipids extracted from yeast (Folch et al., 1957) were used to prepare fatty acid methyl esters (FAMEs) for analysis by gas chromatography as described by Ribes-Navarro et al. (2021). FAMEs were identified and quantified after split-less injection and run in temperature programming, in an Agilent 6850 gas chromatograph system, equipped with a Sapiens-5MS (30 m × 0.25 μm × 0.25 μm) capillary column (Teknokroma Analítica SA, Barcelona, Spain) coupled to a 5975 series mass spectrometer detector (Agilent Technologies, Santa Clara, CA, USA). For the *C. idella* Fads2, conversions of PUFA substrates to the corresponding desaturation products were calculated according to the formula: [individual product area/(all products area + substrate area)] x

Table 1
Primer sets and corresponding PCR conditions used in the cloning of the *C. idella fads2*, *elovl5* and *elovl2* genes.

Gene	Aim	Primer name	Primer sequence	Cycles	Tm	Extension
fads2	Full ORF	CI_fads2_U5F CI_fads2_U3R	CTAAGCAGCAGTCAGTGTTTG TGGATAGTGCTCTGCTTCTC	35	62 °C (10 cycles) 58 °C (25 cycles)	72 °C (1 min)
	Functional characterisation	CI_fads2_VF CI_fads2_VR	CCCAAGCTTAAGATGGGCGGAGGAGGACA CCGCTCGAGTTTATTTGTTGAGGTACGCATCC	35	62 °C (10 cycles) 58 °C (25 cycles)	72 °C (1 min)
elovl2	Full ORF	CI_elovl2_U5F CI_elovl2_U3R	AGCTGTCCCGTATTGTTTAACGG GACGATCCATTCTATTGGTC	35	62 °C (10 cycles) 58 °C (25 cycles)	72 °C (1 min)
	Functional characterisation	CI_elovl2_VF CI_elovl2_VR	CCCAAGCTTAATATGAACCACTTTGAAACG CCGCTCGAGGCATCACTGCAGCTTCTGTT	35	62 °C (10 cycles) 58 °C (25 cycles)	72 °C (1 min)
elovl5	Functional characterisation	CI_elovl5_VF CI_elovl5_VR	CCCAAGCTTAAGATGGAGGCCCTT CCGCTCGAGTCAATCTGCGCG	35	62 °C (10 cycles) 58 °C (25 cycles)	72 °C (1 min)

100. The conversion of substrates 20:3n-3 and 20:2n-6 by Fads2 includes stepwise reactions due to multifunctional desaturation abilities. Thus, it includes the Δ8 desaturation towards 20:4n-3 and 20:3n-6, respectively, and their subsequent Δ5 desaturation to 20:5n-3 and 20:4n-6, respectively. For the *C. idella* Elovl5 and Elovl2, conversions of PUFA substrates to the corresponding elongated products were calculated according to the formula: [areas of all products with longer chain than substrate/(areas of all products with longer chain than substrate + substrate area)] x 100.

2.5. Tracing LC-PUFA metabolism in hepatocytes

Isolated hepatocytes were incubated in the presence of radiolabelled [1-^{14}C] 18:2n-6, [1-^{14}C] 18:3n-3, and [1-^{14}C] 20:5n-3 as described by Rodríguez et al. (2002). Briefly, three specimens of *C. idella* were sacrificed with 0.02% (*v*/v) 2-phenoxyethanol and the liver collected. The liver was then perfused through the hepatic portal vein with a solution of marine Ringer (116 mM NaCl, 6 mM KCl, 1 mM $CaCl_2$, 1 mM $MgSO_4$, 10 mM $NaHCO_3$, 1 mM NaH_2PO_4, 10 mM K_2SO_4 and 10 mM HEPES, at pH 7.4), minced in a Hanks Balanced Salt Solution (HBSS) (NaCl 1.75%, 9.69 mM HEPES, 1.73 mM $NaHCO_3$), and incubated with collagenase at 10 mg mL^{-1} by gently shaking at 20 °C for 40 min. The resultant cell suspension was filtered through a 100 μm nylon mesh with HBSS containing 1% fatty-acid-free bovine serum albumin (FAF-BSA). Cells were collected by centrifugation at 716 *g* for 10 min, washed with HBSS and re-centrifuged for 7 min. The whole process was developed under a cold environment to avoid tissue degradation. Subsequently, each cell preparation was incubated for 3 h with 0.20 μCi of [1-^{14}C] 18:2n-6, [1-^{14}C] 18:3n-3, and [1-^{14}C] 20:5n-3. After incubation, cell viability was assessed by using the trypan blue exclusion test (>90% in all cases). Samples were stored at −80 °C until further analysis.

The protein content of cells was determined according to Lowry et al. (1951) using BSA as standard; total lipid (TL) was extracted according to Folch et al. (1957) updated with the modifications of (Christie and Han, 2010). A 100 μg-aliquot of TL from cells incubated with radiolabelled fatty acid was used to determine radioactivity incorporated using a liquid scintillation β-counter (TRI-CARB 4810TR, Perkin Elmer, Jurong, Singapore). The results obtained in dpm were related to TL and protein contents, and transformed to pmol mg protein^{-1} h^{-1} taking into account the specific activity of each fatty acid.

To determine the capability to biosynthesise LC-PUFA from [1-^{14}C] 18:2n-6, [1-^{14}C]18:3n-3 and [1-^{14}C] 20:5n-3, a 1 mg-aliquot of the TL extract from incubated hepatocytes was transmethylated by acid-catalysis and separated by argentation thin layer chromatography (Christie and Han, 2010). Thin layer chromatography (TLC) plates SIL G-25 (20 cm × 20 cm; Macherey-Nagel GmbH & Co. KG, Düren, Germany) were impregnated with a solution of 2 g silver nitrate in 20 mL acetonitrile followed by activation at 110 °C for 30 min. The plates were totally developed in toluene/acetonitrile (95:5, *v*/v), which resolves the FAMEs into discrete bands based on both chain length and degree of unsaturation (Wilson and Sargent, 1992). Identification of radiolabelled bands was confirmed by radiolabelled standards formulated with a mixture of commercially available [1-^{14}C] fatty acid substrates (18:0, 18:1n-9, 18:2n-6, 18:3n-3, 18:4n-3, 20:4n-6, 20:5n-3 and 22:6n-3) at a concentration of 1 μCi mL^{-1} hexane each, simultaneously run on the same plate (Reis et al., 2019). The TLC plates were developed in toluene/acetonitrile and placed into closed Exposure Cassette-K (Bio-Rad, Madrid, Spain) in contact with a radioactive-sensitive phosphorus screen (Image Screen-K, BioRad) for two weeks. The screens were scanned by an image acquisition system (Molecular Imager FX, BioRad) and the radioactivity of the fatty acid substrates transformed into products was quantified by image analysis software (Image Lab, 6.1.0, BioRad).

3. Results

3.1. Sequences and phylogenetic analysis of fads2, elovl5 and elovl2

The *C. idella fads2*, *elovl5* and *elovl2* ORF of 1335, 876 and 888 bp codify proteins of 444, 291 and 295 aa, respectively. The sequences of *fads2* and *elovl2* were deposited in GenBank database under the accession numbers **OL739359** and **OL739360**, respectively whilst the *elovl5* had already been submitted (**HQ637463.1**).

The *C. idella* Fads2 deduced protein sequence presented all features of a microsomal fatty acyl desaturase, which are three histidine boxes (HXXXH, HXXHH, and QXXHH) and an N-terminal cytochrome *b*5 domain containing the heme-binding motif (HPGG). Furthermore, TMHMM algorithm revealed four transmembrane regions in the grass carp Fads2-like protein (Fig. 2). The *C. idella* Fads2 clustered together with Fads2 from other cyprinids such as tench (*T. tinca*), zebrafish (*D. rerio*) and common carp (*C. carpio*) (Fig. 3).

Both Elovl5 and Elovl2 have a histidine box (HXXHH) in the carboxyl end of the putative protein. Moreover, the *C. idella* Elovl5 deduced protein sequence showed a putative retention signal in the endoplasmic reticulum membrane (Fig. 4). TMHMM algorithm revealed seven transmembrane regions in the *C. idella* Elovl5 (Fig. 4) and five in Elovl2 (Fig. 5). Similar to Fads2, both Elovl5 and Elovl2 from grass carp were closely grouped with corresponding orthologues from zebrafish and tench (Fig. 6).

3.2. Functional characterisation of the C. idella Fads2, Elovl5 and Elovl2 in S. cerevisiae

The ability of the *C. idella* Fads2, Elovl5 and Elovl2 in the LC-PUFA biosynthetic pathways was studied by expressing their ORFs in baker's yeast (*S. cerevisiae*) grown in the presence of desaturase or elongase potential PUFA substrates. Transgenic yeast expressing the *C. idella fads2* exhibited Δ6 desaturase activity since 18:2n-6 and 18:3n-3 were converted to 18:3n-6 and 18:4n-3, respectively (Table 2). Similarly, Δ5 desaturase activity accounting for the conversions of 20:3n-6 and 20:4n-3 to 20:4n-6 and 20:5n-3, respectively, was also detected in yeast expressing the *C. idella fads2* (Table 2). Moreover, this enzyme exhibited Δ8 desaturase activity, with the exogenously added 20:2n-6 and 20:3n-3 being desaturated to 20:3n-6 and 20:4n-3, respectively (Table 2). Interestingly, the *C. idella* Fads2 was demonstrated to also have Δ6 desaturation capacity over 24:5n-3, which was desaturated towards 24:6n-3.

Functional assays of the *C. idella* elongases showed that yeast expressing the *C. idella elovl5* were able to elongate all C_{18} (18:2n-6, 18:3n-3, 18:3n-6 and 18:4n-3) and C_{20} (20:4n-6 and 20:5n-3) PUFA substrates. Among the C_{22} substrates, residual elongation (<1%) was detected for 22:5n-3, but no activity was evident over 22:4n-6 (Table 3). Additionally, yeast expressing the *C. idella elovl2* exhibited elongation ability for all C_{18}, C_{20} and C_{22} PUFA substrates but with relatively higher conversion of 22:5n-3 and 22:4n-6 towards 24:5n-3 and 24:4n-6 (~19%) (Table 3). High affinity of the *C. idella* Elovl2 towards C_{22} PUFAs was further evidenced by the presence of stepwise elongation products of up to C_{28} in yeast expressing the *C. idella elovl2* but not *elovl5* (Table 3).

3.3. Fatty acid metabolism in isolated hepatocytes

Desaturation and elongation activities were recorded in the autoradiographies of lipid extracts from hepatocytes primary cultures incubated with radiolabelled fatty acid ([1-^{14}C] ALA, [1-^{14}C] LA and [1-^{14}C] EPA) (Fig. 7). Our results show that [1-^{14}C] LA (18:2n-6) was desaturated to 18:3n-6 (Δ6 activity), elongated to 20:3n-6 and subsequently desaturated to 20:4n-6 (Δ5 activity) (Fig. 7a). Similarly, ALA (18:3n-3) was desaturated to 18:4n-3 (Δ6 activity), elongated to 20:4n-3 and desaturated to 20:5n-3 (Δ5 activity) (Fig. 7b). Moreover, incubation of

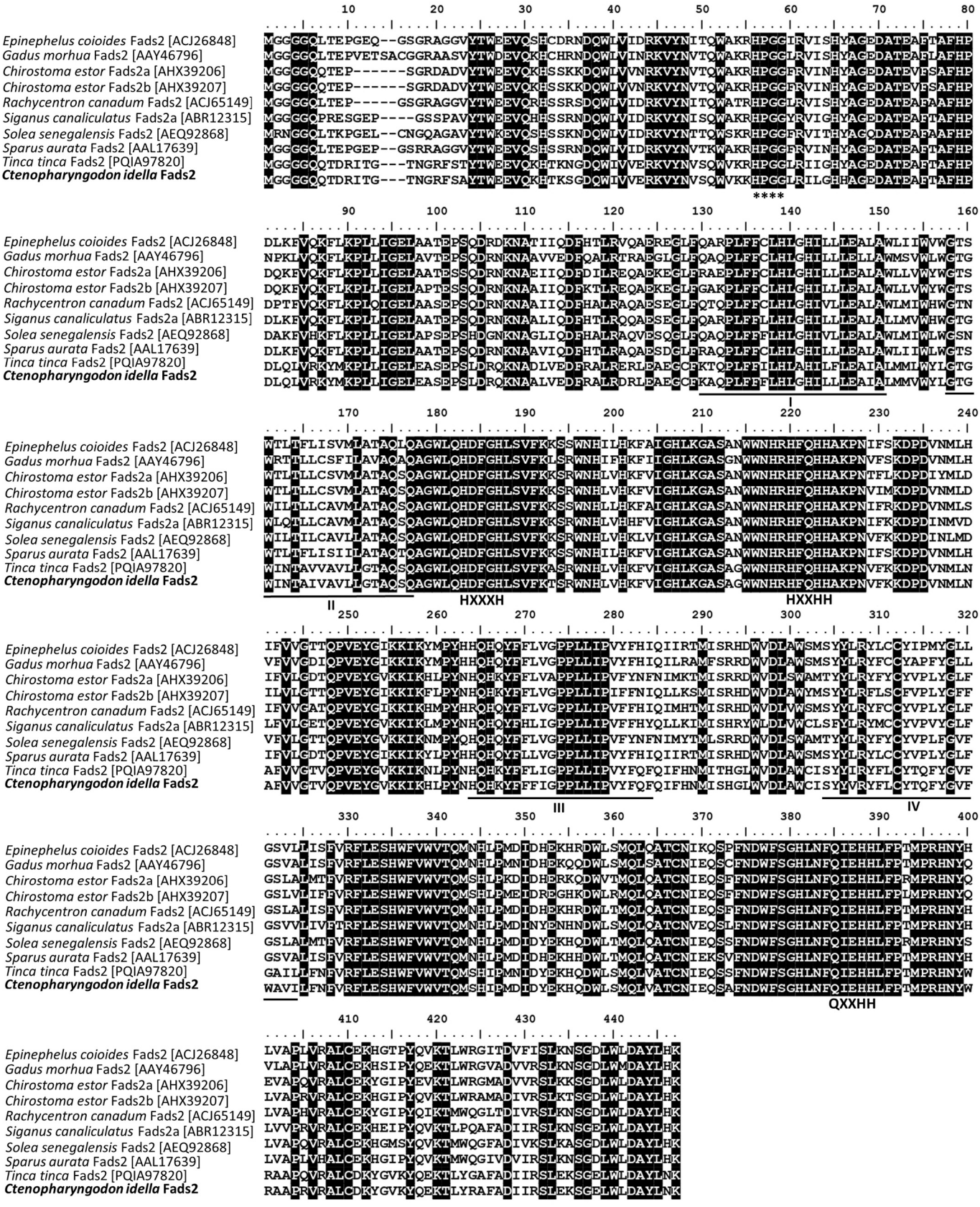

Fig. 2. Comparison of Fads2 deduced amino acid sequence from *Ctenopharyngodon idella* with other telosts species. *C. idella* Fads2 contained heme-biding motif (HPGG) and three histidine boxes (HXXXH, HXXHH and QXXHH), which are conserved in the Fads family. Four putative membrane-spanning domains are underlined.

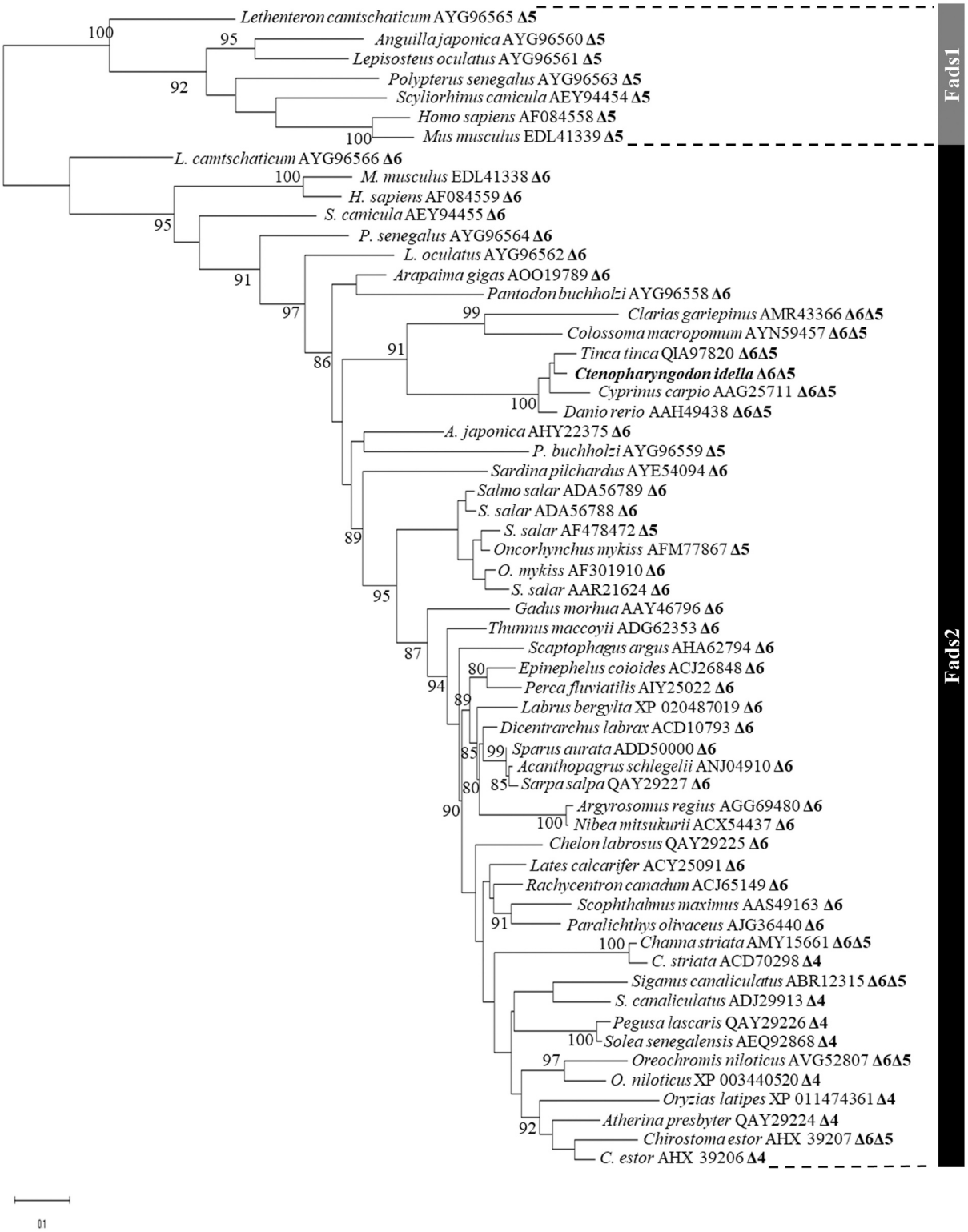

Fig. 3. Phylogenetic tree of Fads2 using the deduced amino acid sequences from grass carp (*Ctenopharyngodon idella*). The horizontal branch length is proportional to the amino acid substitution rate per site. Demonstrated desaturase activities are included in all Fads-like sequence as "Δx". Accession numbers according to the NCBI database are included for each sequence. The transfer distance bootstrap support value (%) is given in each node. Values lower than 80% are not shown.

hepatocytes with [1-^{14}C] EPA (20:5n-3) resulted in two elongation products (22:5n-3 and 24:5n-3), and the desaturated product 24:6n-3 (Δ6 activity) (Fig. 7c). [1-^{14}C] 20:5n-3 was the most incorporated radiolabelled fatty acid in hepatocytes (73.6 ± 25.53 pmol mg prot^{-1} h^{-1}), compared to the two [1-$^{14}C_{18}$] fatty acid (18:2n-6 and 18:3n-3; 48.15 ± 5.59 and 32.53 ± 2.81 pmol mg prot^{-1} h^{-1}, respectively) (Table 4). The transformation proportion of radiolabelled substrates was 14.31 ± 8.29% for [1-^{14}C] 18:3n-3, 11.07 ± 2.50% for [1-^{14}C] 18:2n-6, and 9.37 ± 3.48% for [1-^{14}C] 20:5n-3 (Table 5). [1-^{14}C] 18:2n-6 and [1-^{14}C] 18:3n-3 showed desaturation activities in all three fish, but

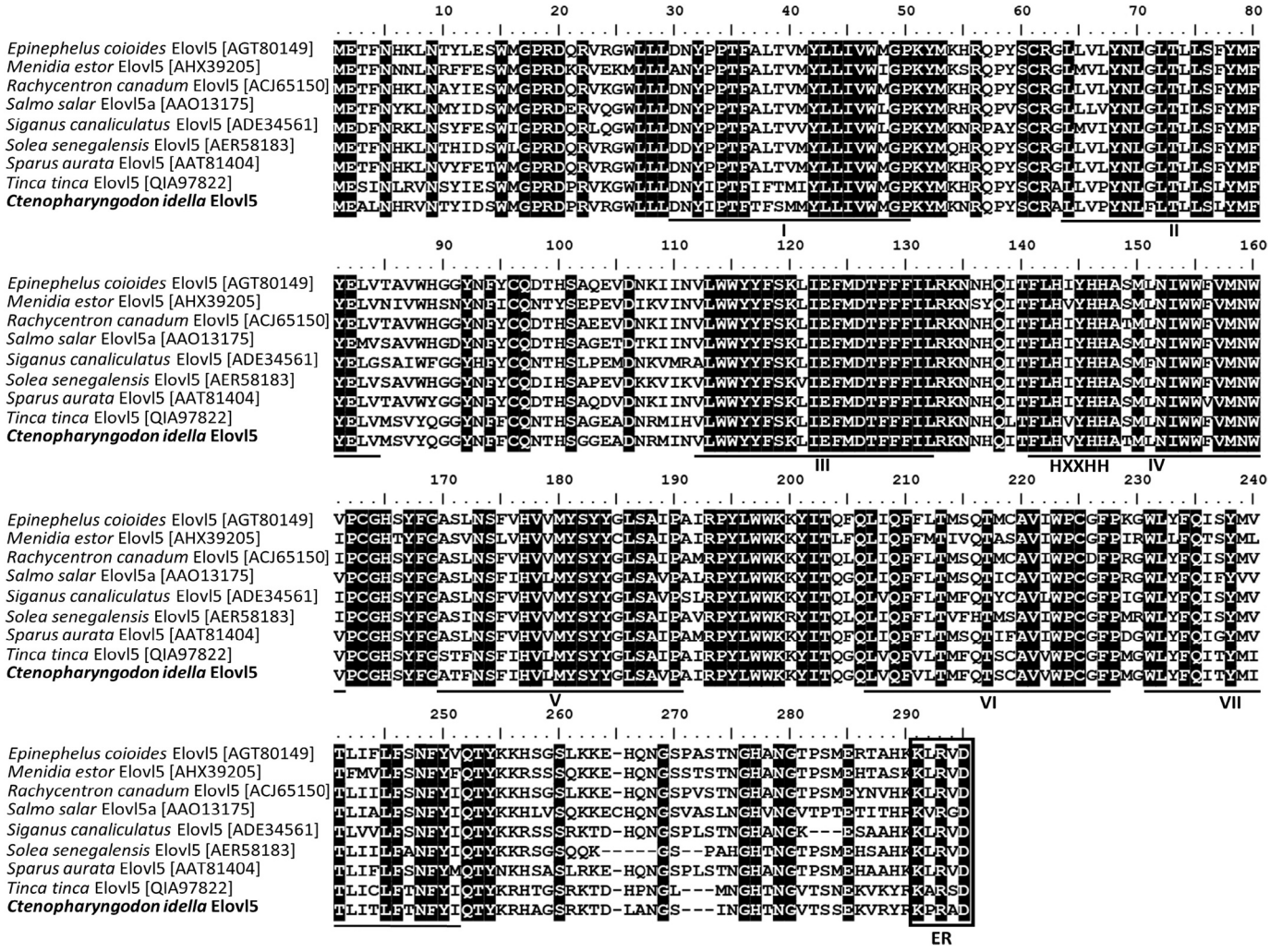

Fig. 4. Comparison of Elovl5 deduced amino acid sequence from *Ctenopharyngodon idella* with other telosts species. Identical residues are shaded black. *C. idella* Elovl5 contained histidine box (HXXHH) and endoplasmic reticulum retrieval signal (KXRXD). Seven putative membrane-spanning domains are underlined.

[1-^{14}C] 20:5n-3 only showed desaturation activity, from 24:5n-3 to 24:6n-3, in one out of three.

4. Discussion

There is increasing interest in understanding the capacity of farmed teleosts to biosynthesise LC-PUFAs from their C_{18} PUFA precursors in order to predict their ability to efficiently utilise VOs included in their diets. The repertoire of enzymes, namely fatty acyl desaturases and elongases, necessary to produce ARA, EPA and DHA from LA and ALA, has been already characterised in several teleost species (Xie et al., 2021; Turchini et al., 2022). In this context, cyprinids including *D. rerio* (Hastings et al., 2001), *T. tinca* (Garrido et al., 2020) and *Barbonymus gonionotus* (Janaranjani et al., 2018) have been reported to possess the entire enzymatic machinery for the biosynthesis of LC-PUFA from C_{18} substrates. However, a complete characterisation of this biosynthetic ability in grass carp, *C. idella*, the most common freshwater farmed fish species with 5.7 million tonnes per year produced worldwide (Jiang et al., 2015; FAO, 2020), is largely lacking, and has been only partly addressed by Xie et al. (2020). Our study provides molecular and metabolic evidences demonstrating that grass carp shows all the desaturase and elongase activities required to convert the dietary essential LA and ALA into the biologically important ARA, EPA and DHA.

The Δ6, Δ5 and Δ8 desaturase activities of grass carp Fads2 illustrate the diversity of pathways that this species can operate to efficiently utilise dietary C_{18} PUFA. Our results confirm the function as Δ6 desaturases towards LA and ALA of Fads2 from *C. idella* previously stated by Xie et al. (2020). Importantly, we herein provide evidences that, along the Δ6 activity towards C_{18} substrates, *C. idella* Fads2 also operates as Δ6 towards 24:5n-3, which can be converted to 24:6n-3, establishing its potential to proceed through the so called "Sprecher pathway" (Sprecher, 2000). These results are in agreement with those reported in the cyprinid *D. rerio* (Tocher et al., 2003; Oboh et al., 2017), as well as in the silurid African catfish *C. gariepinus* (Oboh et al., 2016). In addition, the lack of activity of *C. idella* Fads2 towards 22:5n-3 and 22:4n-6 confirmed that this enzyme does not have Δ4 desaturase capacity, indicating that DHA can only occur *via* the Sprecher pathway. Consistently, Δ4 Fads2 have not yet been identified in other cyprinids (Hastings et al., 2001; Zheng et al., 2004; Janaranjani et al., 2018; Garrido et al., 2020) suggesting that such enzymatic ability is probably absent in early emerged teleosts like cyprinids (Oboh et al., 2017).

Along the Δ6 desaturase activity, our functional characterisation assays proved for the first time the function as Δ8 and Δ5 desaturases of Fads2 from *C. idella*. Other Fads2 with Δ6, Δ5 and Δ8 activities have been previously described in several freshwater fish species (Fonseca-Madrigal et al., 2014; Kuah et al., 2016; Oboh et al., 2016), including cyprinids such as *D. rerio* (Hastings et al., 2001; Monroig et al., 2011) and *B. gonionotus* (Janaranjani et al., 2018). Contrarily, other cyprinids such as *T. tinca* and *C. carpio* have Fads2 with Δ6 and Δ5 but no Δ8 desaturase activities (Zheng et al., 2004; Garrido et al., 2020).

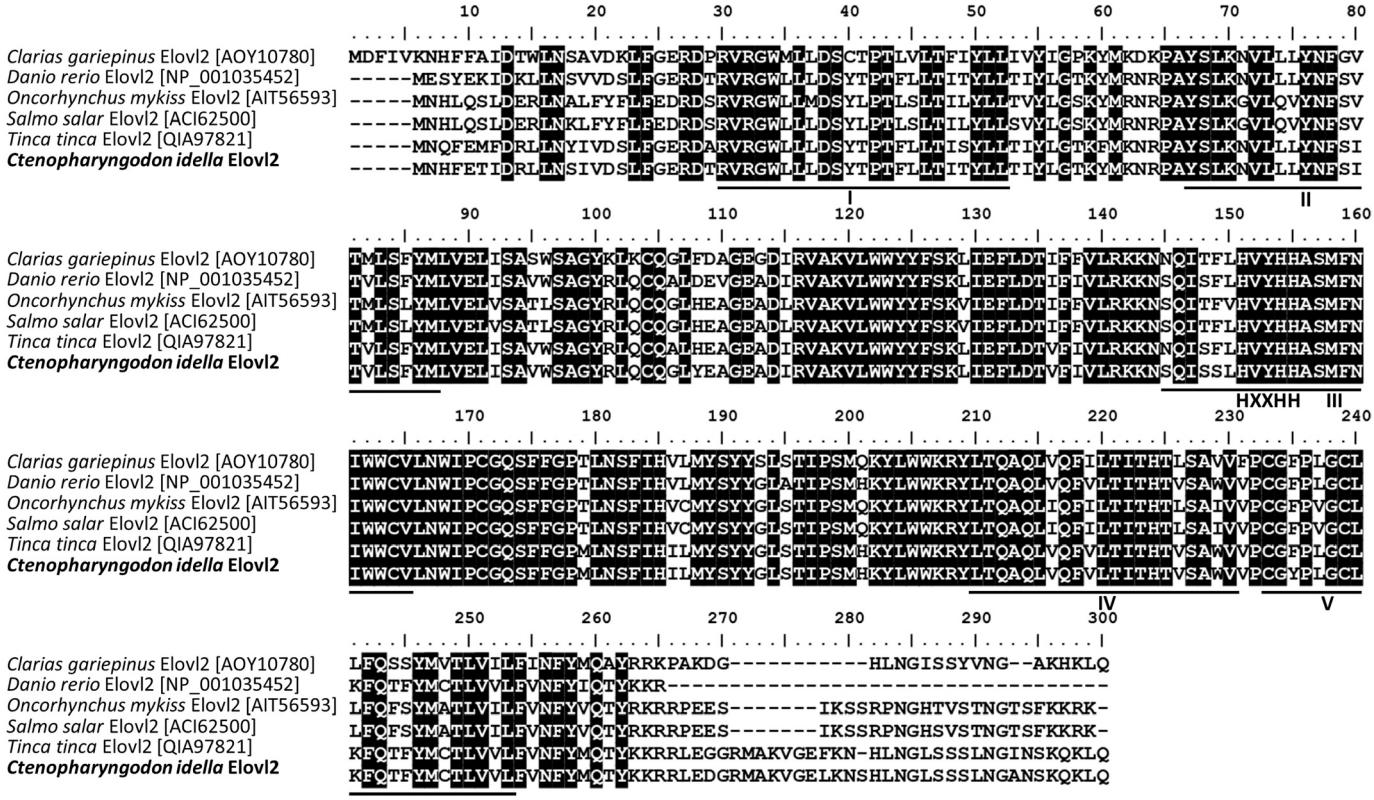

Fig. 5. Comparison of Elovl2 deduced amino acid sequence from *Ctenopharyngodon idella* with other telosts species. Identical residues are shaded black. *C. idella* Elovl5 contained histidine box (HXXHH). Five putative membrane-spanning domains are underlined.

Collectively, the desaturase activities of Fads2 from cyprinids enable all the desaturation reactions required to biosynthesise ARA and EPA from LA and ALA, respectively (Fig. 1). However, whereas *T. tinca* and *C. carpio* would be only able to operate the Δ6 pathway (Δ6 desaturation – elongation – Δ5 desaturation), other teleosts including *C. idella* can proceed through both the Δ6 and the Δ8 pathways (elongation – Δ8 desaturation –Δ5 desaturation) (Monroig et al., 2011). Interestingly, our results clearly show that the two PUFA elongases characterised from *C. idella* ensure the elongation required in both pathways for the biosynthesis of ARA and EPA.

In agreement with other Elovl5-like proteins from teleosts (Morais et al., 2012; Monroig et al., 2013; Kuah et al., 2015; Janaranjani et al., 2018; Ferraz et al., 2019; Garrido et al., 2020; Galindo et al., 2021), the grass carp Elovl5 was found to be active towards both C_{18} and C_{20} substrates enabling all the necessary elongations to obtain ARA and EPA. Unlike Elovl5, Elovl2 is not present in all teleosts (Monroig et al., 2016) and it appears to be lost in Acanthopterygii, a phylogenetic group that includes the vast majority of the most important farmed marine fish species (Castro et al., 2016). However, species from earlier emerged teleost lineages such as cyprinids (Monroig et al., 2009; Garrido et al., 2020), silurids (Oboh et al., 2016), serrasalmid (Ferraz et al., 2019), clupeid (Machado et al., 2018) and salmonids (Morais et al., 2009) possess functional Elovl2 enzymes. Consistently, the grass carp Elovl2 elongated C_{18}, C_{20} and C_{22} substrates. While the elongation capacity towards C_{18} and C_{20} PUFAs is somewhat overlapping with that of the afore-mentioned grass carp Elovl5, the efficiency of Elovl2 over C_{22} PUFAs, particularly 22:5n-3, highlights its essential role in the biosynthesis of DHA since it allows the production of 24:5n-3, a key intermediate of the Sprecher pathway. Thus, the consecutive action of the Elovl2 producing 24:5n-3, and the subsequent Δ6 desaturation to 24:6n-3 by Fads2 shown in the present study, demonstrates that a complete enzymatic capacity for DHA biosynthesis exists in grass carp.

The functions of individual desaturase and elongase genes derived from the yeast-based assay are consistent with the assays of enzymatic activity performed on hepatocytes incubated with radiolabelled substrates. Indeed, these metabolic experiments further confirmed that grass carp has functional and active Δ6 and Δ5 desaturase capacities to obtain ARA and EPA from LA and ALA, as well as to elongate EPA to 22:5n-3 and 24:5n-3, and to desaturate the latter towards 24:6n-3 through Δ6 desaturation (Fig. 7c), as pointed out by functional characterisation in yeast.

Despite no DHA was recovered in our metabolic assays, the presence of 24:6n-3 provides direct evidence for the activation of the Sprecher pathway for its production (Oboh et al., 2017). In agreement with our results, hepatocytes from rainbow trout (Buzzi et al., 1997) incubated for 3 h with radiolabelled 20:5n-3, produced 22:5n-3, 24:5n-3 and 24:6n-3 but not DHA. However, when enterocytes and hepatocytes from *T. tinca*, which possess a similar enzyme repertoire that *C. idella*, were incubated for 3 h with radiolabelled 18:3n-3, residual amounts of DHA were recovered in hepatocytes, and both 24:6n-3 and DHA in enterocytes (Garrido et al., 2020). Contrarily, DHA but not 24:6n-3 was obtained in similar assays with both cell types from the flatfish *Pegusa lascaris* (Galindo et al., 2021), which possesses Δ4 Fads2 (Garrido et al., 2019), suggesting the desaturation of 22:5n-3 to DHA through the direct Δ4 pathway instead of through the Sprecher one (Galindo et al., 2021). Therefore, all discussed above indicate that Δ6 desaturase ability to transform 24:5n-3 to 24:6n-3 is the key step required for DHA biosynthesis *via* the Sprecher pathway.

5. Conclusions

In conclusion, the combination of the functional characterisation and enzymatic activity assays demonstrated that grass carp *C. idella* shows all the desaturase and elongase activities required to convert LA into ARA, and ALA into EPA and DHA. These results strongly suggest that grass carp can satisfy its essential LC-PUFA requirements with an

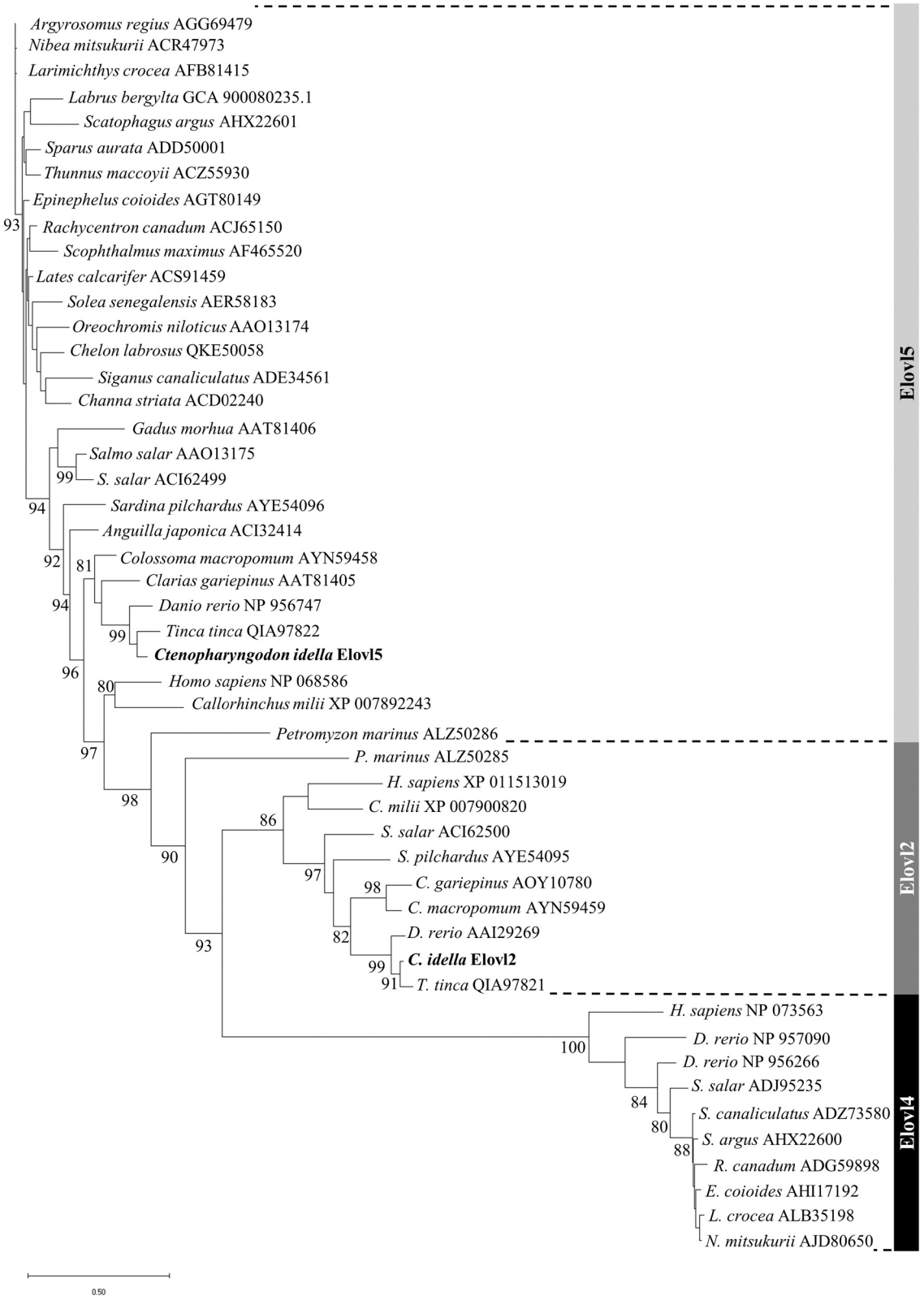

Fig. 6. Phylogenetic tree of Elovl2 and Elovl5 using the deduced amino acid sequences from grass carp (*Ctenopharyngodon idella*). The horizontal branch length is proportional to the amino acid substitution rate per site. Accession numbers according to the NCBI database are included for each sequence. The transfer distance bootstrap support value (%) is given in each node. Values lower than 80% are not shown.

Table 2
Functional characterisation of the grass carp Fads2. Individual conversion (%) of polyunsaturated fatty acid substrates are presented as [individual product area/(all products area + substrate area)] x 100.

		Conversion (%)	
Substrate	Product	Fads2	Activity
18:3n-3	18:4n-3	3.6	Δ6
18:2n-6	18:3n-6	1.8	Δ6
20:3n-3	20:4n-3	2.0 [a]	Δ8
20:2n-6	20:3n-6	0.3[a]	Δ8
20:4n-3	20:5n-3	1.3	Δ5
20:3n-6	20:4n-6	0.8	Δ5
22:5n-3	nd	nd	nd
22:4n-6	nd	nd	nd
24:5n-3	24:6n-3	0.8	Δ6

[a] Conversions towards 20:3n-3 and 20:2n-6 substrates by Fads2 include stepwise reactions due to multifunctional desaturation abilities. Thus, the conversion of the grass carp Fads2 on 20:3n-3 and 20:2n-6 includes the Δ8 desaturation towards 20:4n-3 and 20:3n-6, respectively, and their subsequent Δ5 desaturation to 20:5n-3 and 20:4n-6, respectively. nd, not detected.

Table 3
Functional characterisation of the grass carp Elovl5 and Elovl2 in yeast. Conversion (%) of polyunsaturated fatty acid substrates were calculated according to the formula [areas of all products with longer chain than substrate/(areas of all products with longer chain than substrate + substrate area)] x 100. The conversion of intermediary products along the elongation pathway is also shown.

		Conversion (%)		
Substrate	Product	Elovl5	Elovl2	Activity
18:3n-3	20:3n-3	17.7	9.3	C18 → C20
18:2n-6	20:2n-6	13.2	1.2	C18 → C20
	20:4n-3	65.6	14.1	C18 → C20
18:4n-3	22:4n-3	3.1	6.2	C20 → C22
	24:4n-3	nd	2.3	C22 → C24
	26:4n-3	nd	0.1	C24 → C26
	20:3n-6	57.1	8.0	C18 → C20
18:3n-6	22:3n-6	0.9	1.3	C20 → C22
	24:3n-6	nd	0.6	C22 → C24
	26:3n-6	nd	0.1	C24 → C26
	22:5n-3	44.7	9.9	C20 → C22
20:5n-3	24:5n-3	0.4	58.5	C22 → C24
	26:5n-3	nd	2.7	C24 → C26
	28:5n-3	nd	0.1	C26 → C28
	22:4n-6	31.3	2.9	C20 → C22
20:4n-6	24:4n-6	nd	38.0	C22 → C24
	26:4n-6	nd	1.9	C24 → C26
	28:4n-6	nd	0.2	C26 → C28
	24:5n-3	0.6	18.9	C22 → C24
22:5n-3	26:5n-3	nd	0.9	C24 → C26
	28:5n-3	nd	0.1	C26 → C28
	24:4n-6	nd	17.7	C22 → C24
22:4n-6	26:4n-6	nd	1.4	C24 → C26
	28:4n-6	nd	0.3	C26 → C28

nd, not detected.

adequate supply of C_{18} PUFAs in the diet. This novel knowledge could be of great interest to aquafeed manufacturers in order to reduce the dietary inclusion of FO and, hence the production costs of this important aquaculture species while maintaining its nutritional value for consumers.

Funding

This study was funded by the Ministry of Science, Innovation and Universities, Spanish Government (AGL2015–70994-R; PROPUFAW3); Agencia Canaria de Investigación, Innovación y Sociedad de la Información, Consejería de Economía, Conocimiento y Empleo and Fondo Social Europeo (FSE) Programa Operativo Integrado de Canarias

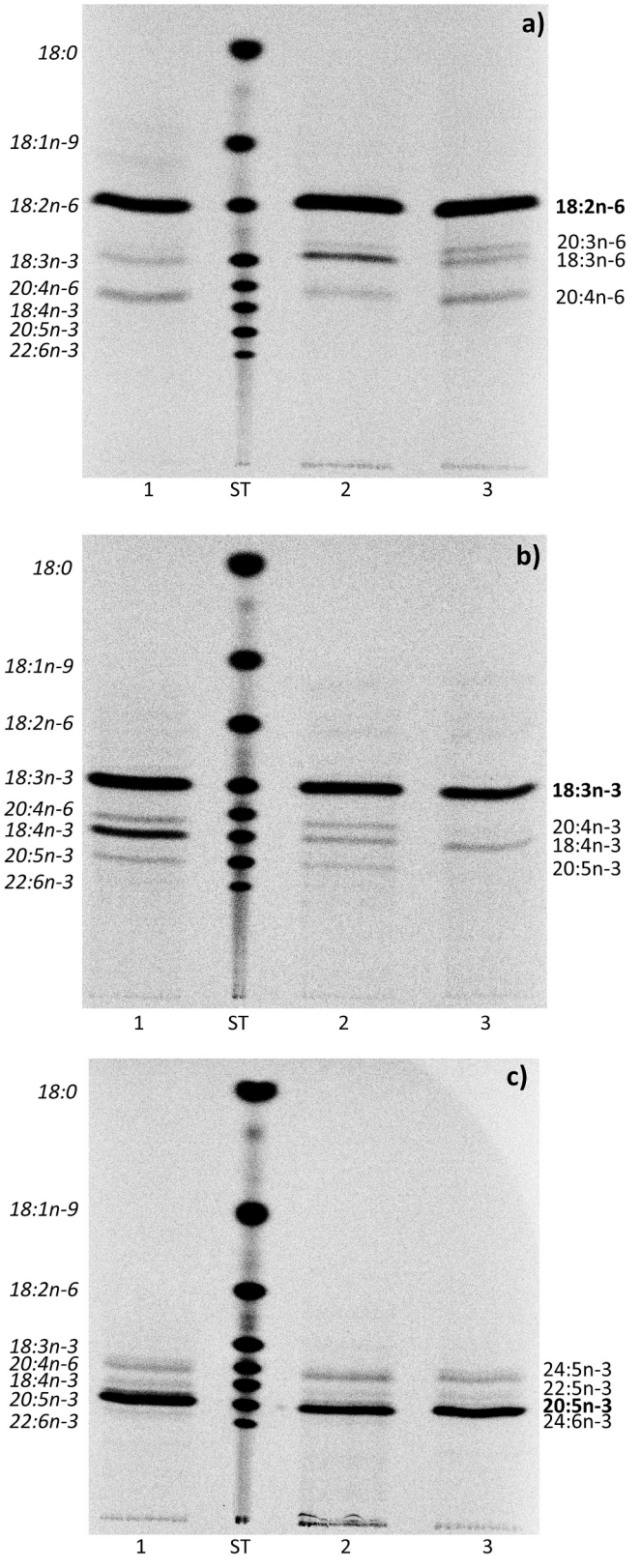

Fig. 7. Autoradiography of TLC plate-developed radiolabelled fatty acids prepared from hepatocytes of each single grass carp specimen ($n = 3$). The standard mixture of fatty acid methyl esters (ST) in italics (left side), [1-^{14}C] substrate in bold and products (right side). Hepatocytes were incubated with three radiolabelled fatty acids: a) [1-^{14}C] 18:3n-3, b) [1-^{14}C] 18:2n-6 and c) [1-^{14}C] 20:5n-3.

Table 4
Incorporation of radioactivity into total lipids (pmol mg prot^{-1} h^{-1}) and bioconversions (% of total radioactivity) registered in isolated hepatocytes incubated with [1-^{14}C] 18:2n-6, [1-^{14}C] 18:3n-3 and [1-^{14}C] 20:5n-3.

[1–^{14}C] 18:2n-6	**1**	**2**	**3**
Incorporation	42.32	53.47	48.66
FA recovery	86.40	89.00	91.40
Elongation	nd	0.50	1.00
Desaturation	3.80	7.90	2.30
E + D	9.80	2.60	5.20
[1–^{14}C] 18:3n-3	**1**	**2**	**3**
Incorporation	29.57	32.88	35.15
FA recovery	76.39	88.39	92.30
Elongation	nd	nd	nd
Desaturation	18.26	5.50	7.70
E + D	5.35	6.11	nd
[1–^{14}C] 20:5n-3	**1**	**2**	**3**
Incorporation	102.98	61.01	56.82
FA recovery	93.90	86.90	91.20
Elongation	5.60	13.10	8.80
Desaturation	nd	nd	nd
E + D	0.50	nd	nd

E + D, products which combine elongation and desaturation processes; nd, not detected.

Table 5
Products obtained (% of total radioactivity) from the incubation of isolated hepatocytes with [1-^{14}C] 18:2n-6, [1-^{14}C] 18:3n-3 and [1-^{14}C] 20:5n-3.

	1	**2**	**3**
[1–^{14}C] 18:2n-6	86.40	89.00	91.40
18:3n-6	3.80	7.90	2.30
20:3n-6	nd	0.50	1.00
20:4n-6	9.80	2.60	5.20
[1–^{14}C] 18:3n-3	76.39	88.39	92.30
18:4n-3	18.26	5.50	7.70
20:4n-3	2.52	3.46	nd
20:5n-3	2.83	2.65	nd
[1–^{14}C] 20:5n-3	93.90	86.90	91.20
22:5n-3	0.70	0.80	1.10
24:5n-3	4.90	12.30	7.70
24:6n-3	0.50	nd	nd

nd, not detected.

2014–2020, Eje 3 Tema Prioritario 74 (85%) (PhD contract M.M.), and CajaSiete (PhD contract A.G.). C. Rodríguez is a member of the Instituto de Tecnologías Biomédicas (ITB) de Canarias.

Declaration of Competing Interest

The authors declare that they have no known competing financial interests or personal relationships that could have appeared to influence the work reported in this paper.

Acknowledgements

The authors appreciate the collaboration of Fundación Neotrópico to provide *C. idella* specimens.

References

Barceló-Coblijn, G., Murphy, E.J., 2009. Alpha-linolenic acid and its conversion to longer chain n-3 fatty acids: benefits for human health and a role in maintaining tissue n-3 fatty acid levels. Prog. Lipid Res. 48, 355–374. https://doi.org/10.1016/j.plipres.2009.07.002.

Buzzi, M., Henderson, R.J., Sargent, J.R., 1997. Biosynthesis of docosahexaenoic acid in trout hepatocytes proceeds via 24-carbon intermediates. Comp. Biochem. Physiol. Part B Biochem. Mol. Biol. 116, 263–267. https://doi.org/10.1016/S0305-0491(96)00210-6.

Castro, L.F.C., Tocher, D.R., Monroig, O., 2016. Long-chain polyunsaturated fatty acid biosynthesis in chordates: insights into the evolution of fads and Elovl gene repertoire. Prog. Lipid Res. 62, 25–40. https://doi.org/10.1016/j.plipres.2016.01.001.

Christie, W.W., Han, X., 2010. Lipid Analysis: Isolation, Separation, Identification and Lipidomic Analysis. Oily Press. an Impr. PJ Barnes Assoc, pp. 55–66.

Darriba, Di, Posada, D., Kozlov, A.M., Stamatakis, A., Morel, B., Flouri, T., 2020. ModelTest-NG: a new and scalable tool for the selection of DNA and protein evolutionary models. Mol. Biol. Evol. 37, 291–294. https://doi.org/10.1093/molbev/msz189.

FAO, 2020. The State of World Fisheries and Aquaculture 2020: Sustainability in Action. Food and Agriculture Organisation of the United Nations, Rome, Italy. https://doi.org/10.4060/ca9229en.

Ferraz, R.B., Kabeya, N., Lopes-Marques, M., Machado, A.M., Ribeiro, R.A., Salaro, A.L., Ozório, R., Castro, L.F.C., Monroig, Ó., 2019. A complete enzymatic capacity for long-chain polyunsaturated fatty acid biosynthesis is present in the Amazonian teleost tambaqui, *Colossoma macropomum*. Comp. Biochem. Physiol. Part B Biochem. Mol. Biol. 227, 90–97. https://doi.org/10.1016/j.cbpb.2018.09.003.

Folch, J., Lees, M., Stanley, G.H.S., 1957. A simple method for the isolation and purification of total lipides from animal tissues. J. Biol. Chem. 226, 497–509.

Fonseca-Madrigal, J., Pineda-Delgado, D., Martínez-Palacios, C., Rodríguez, C., Tocher, D.R., 2012. Effect of salinity on the biosynthesis of n-3 long-chain polyunsaturated fatty acids in silverside *Chirostoma estor*. Fish Physiol. Biochem. 38, 1047–1057. https://doi.org/10.1007/s10695-011-9589-6.

Fonseca-Madrigal, J., Navarro, J.C., Hontoria, F., Tocher, D.R., Martínez-Palacios, C.A., Monroig, Ó., 2014. Diversification of substrate specificities in teleostei Fads2: characterization of Δ4 and Δ6Δ5 desaturases of *Chirostoma estor*. J. Lipid Res. 55, 1408–1419. https://doi.org/10.1194/jlr.M049791.

Galindo, A., Garrido, D., Monroig, Ó., Pérez, J.A., Betancor, M.B., Acosta, N.G., Kabeya, N., Marrero, M.A., Bolaños, A., Rodríguez, C., 2021. Polyunsaturated fatty acid metabolism in three fish species with different trophic level. Aquaculture 530, 735761. https://doi.org/10.1016/j.aquaculture.2020.735761.

Garrido, D., Kabeya, N., Betancor, M.B., Pérez, J.A., Acosta, N.G., Tocher, D.R., Rodríguez, C., Monroig, Ó., 2019. Functional diversification of teleost Fads2 fatty acyl desaturases occurs independently of the trophic level. Sci. Rep. 9, 11199. https://doi.org/10.1038/s41598-019-47709-0.

Garrido, D., Monroig, O., Galindo, A., Betancor, M.B., Perez, J.A., Kabeya, N., Marrero, M., Rodriguez, C., 2020. Lipid metabolism in *Tinca tinca* and its n-3 LC-PUFA biosynthesis capacity. Aquaculture 523, 735147. Doi:10.1016/j.aquaculture.2020.735147.

Gladyshev, M.I., Sushchik, N.N., Makhutova, O.N., 2013. Production of EPA and DHA in aquatic ecosystems and their transfer to the land. Prostaglandins Other Lipid Mediat. 107, 117–126. https://doi.org/10.1016/j.prostaglandins.2013.03.002.

Guillou, H., Zadravec, D., Martin, P.G.P., Jacobsson, A., 2010. The key roles of elongases and desaturases in mammalian fatty acid metabolism: insights from transgenic mice. Prog. Lipid Res. 49, 186–199. https://doi.org/10.1016/j.plipres.2009.12.002.

Hastings, N., Agaba, M., Tocher, D.R., Leaver, M.J., Dick, J.R., Sargent, J.R., Teale, A.J., 2001. A vertebrate fatty acid desaturase with Δ5 and Δ6 activities. Proc. Natl. Acad. Sci. 98, 14304–14309. https://doi.org/10.1073/pnas.251516598.

Hixson, S.M., 2014. Fish nutrition and current issues in aquaculture: the balance in providing safe and nutritious seafood, in an environmentally sustainable manner. J. Aquac. Res. Dev. 5 https://doi.org/10.4172/2155-9546.1000234.

Innes, J.K., Calder, P.C., 2018. The differential effects of eicosapentaenoic acid and docosahexaenoic acid on cardiometabolic risk factors: a systematic review. Int. J. Mol. Sci. 19 https://doi.org/10.3390/ijms19020532.

Ishikawa, A., Kabeya, N., Ikeya, K., Kakioka, R., Cech, J.N., Osada, N., Leal, M.C., Inoue, J., Kume, M., Toyoda, A., Tezuka, A., Nagano, A.J., Yamasaki, Y.Y., Suzuki, Y., Kokita, T., Takahashi, H., Lucek, K., Marques, D., Takehana, Y., Naruse, K., Mori, S., Monroig, O., Ladd, N., Schubert, C.J., Matthews, B., Peichel, C. L., Seehausen, O., Yoshizaki, G., Kitano, J., 2019. A key metabolic gene for recurrent freshwater colonization and radiation in fishes. Science 364, 886–889. https://doi.org/10.1126/science.aau5656.

Jakobsson, A., Westerberg, R., Jacobsson, A., 2006. Fatty acid elongases in mammals: their regulation and roles in metabolism. Prog. Lipid Res. 45, 237–249. https://doi.org/10.1016/j.plipres.2006.01.004.

Janaranjani, M., Mah, M., Kuah, M., Fadhilah, N., Hing, S., 2018. Capacity for eicosapentaenoic acid and arachidonic acid biosynthesis in silver barb (*Barbonymus gonionotus*): functional characterisation of a Δ6/Δ8/Δ5 Fads2 desaturase and Elovl5 elongase. Aquaculture 497, 469–486. https://doi.org/10.1016/j.aquaculture.2018.08.019.

Jiang, X., Xu, Y., Ge, L., Xia, W., Jiang, Q., 2015. Original Article the Impact of Collagen on Softening of Grass Carp (*Ctenopharyngodon idella*) Fillets Stored under Superchilled and Ice Storage 2427–2435. https://doi.org/10.1111/ijfs.12909.

Kuah, M.-K., Jaya-Ram, A., Shu-Chien, A.C., 2015. The capacity for long-chain polyunsaturated fatty acid synthesis in a carnivorous vertebrate: functional characterisation and nutritional regulation of a Fads2 fatty acyl desaturase with Δ4 activity and an Elovl5 elongase in striped snakehead (*Channa striata*). Biochim. Biophys. Acta Mol. Cell Biol. Lipids 1851, 248–260. https://doi.org/10.1016/j.bbalip.2014.12.012.

Kuah, M.-K., Jaya-Ram, A., Shu-Chien, A.C., 2016. A fatty acyl desaturase (fads2) with dual Δ6 and Δ5 activities from the freshwater carnivorous striped snakehead *Channa*

striata. Comp. Biochem. Physiol. A. Mol. Integr. Physiol. 201, 146–155. https://doi.org/10.1016/j.cbpa.2016.07.007.

Lauritzen, L., Hansen, H.S., Jorgensen, M.H., Michaelsen, K.F., 2001. The essentiality of long chain n-3 fatty acids in relation to development and function of the brain and retina. Prog. Lipid Res. 40, 1–94. https://doi.org/10.1016/S0163-7827(00)00017-5.

Lemoine, F., Domelevo Entfellner, J.B., Wilkinson, E., Correia, D., Dávila Felipe, M., De Oliveira, T., Gascuel, O., 2018. Renewing Felsenstein's phylogenetic bootstrap in the era of big data. Nature 556, 452–456. https://doi.org/10.1038/s41586-018-0043-0.

Lopes-Marques, M., Kabeya, N., Qian, Y., Ruivo, R., Santos, M.M., Venkatesh, B., Tocher, D.R., Castro, L.F.C., Monroig, Ó., 2018. Retention of fatty acyl desaturase 1 (fads1) in Elopomorpha and Cyclostomata provides novel insights into the evolution of long-chain polyunsaturated fatty acid biosynthesis in vertebrates. BMC Evol. Biol. 18, 1–9. https://doi.org/10.1186/s12862-018-1271-5.

Lowry, O.H., Rosebrough, N.J., Farr, A.L., Randall, R.J., 1951. Protein measurement with the Folin phenol reagent. J. Biol. Chem. 193, 265–275.

Luo, J., Monroig, Ó., Liao, K., Ribes-Navarro, A., Navarro, J.C., Zhu, T., Li, J., Xue, L., Zhou, Q., Jin, M., 2021. Biosynthesis of LC-PUFAs and VLC-PUFAs in *Pampus argenteus*: characterization of Elovl4 Elongases and regulation under acute salinity. J. Agric. Food Chem. https://doi.org/10.1021/acs.jafc.0c06277.

Lutteropp, S., Kozlov, A.M., Stamatakis, A., 2020. A fast and memory-efficient implementation of the transfer bootstrap. Bioinformatics 36, 2280–2281. https://doi.org/10.1093/bioinformatics/btz874.

Machado, A.M., Tørresen, O.K., Kabeya, N., Couto, A., Petersen, B., Felício, M., Campos, P.F., Fonseca, E., Bandarra, N., Lopes-Marques, M., Ferraz, R., Ruivo, R., Fonseca, M.M., Jentoft, S., Monroig, Ó., Da Fonseca, R.R., Castro, C., L.F, 2018. "Out of the can": a draft genome assembly, liver transcriptome, and nutrigenomics of the European sardine, *Sardina pilchardus*. Genes (Basel). https://doi.org/10.3390/genes9100485.

Mallick, R., Basak, S., Duttaroy, A.K., 2019. Docosahexaenoic acid, 22:6n-3: its roles in the structure and function of the brain. Int. J. Dev. Neurosci. 79, 21–31. https://doi.org/10.1016/j.ijdevneu.2019.10.004.

Marrero, M., Monroig, Ó., Betancor, M., Herrera, M., Pérez, J.A., Garrido, D., Galindo, A., Giráldez, I., Rodríguez, C., 2021. Influence of dietary lipids and environmental salinity on the n-3 long-chain polyunsaturated fatty acids biosynthesis capacity of the marine teleost *Solea senegalensis*. Mar. Drugs 19. https://doi.org/10.3390/md19050254.

Miller, M.A., Pfeiffer, W., Schwartz, T., 2010. Creating the CIPRES Science Gateway for inference of large phylogenetic trees. In: Gatew. Comput. Environ. Work. GCE. https://doi.org/10.1109/GCE.2010.5676129.

Monroig, Ó., Kabeya, N., 2018. Desaturases and elongases involved in polyunsaturated fatty acid biosynthesis in aquatic invertebrates: a comprehensive review. Fish. Sci. 84, 911–928. https://doi.org/10.1007/s12562-018-1254-x.

Monroig, Ó., Rotllant, J., Sánchez, E., Cerdá-reverter, J.M., Tocher, D.R., 2009. Biochimica et Biophysica Acta expression of long-chain polyunsaturated fatty acid (LC-PUFA) biosynthesis genes during zebra fish *Danio rerio* early embryogenesis. BBA - Mol. Cell Biol. Lipids 1791, 1093–1101. https://doi.org/10.1016/j.bbalip.2009.07.002.

Monroig, Ó., Li, Y., Tocher, D.R., 2011. Delta-8 desaturation activity varies among fatty acyl desaturases of teleost fish: high activity in delta-6 desaturases of marine species. Comp. Biochem. Physiol. Part B 159, 206–213. https://doi.org/10.1016/j.cbpb.2011.04.007.

Monroig, Ó., Tocher, D.R., Hontoria, F., Navarro, J.C., 2013. Functional characterisation of a Fads2 fatty acyl desaturase with Δ6/Δ8 activity and an Elovl5 with C_{16}, C_{18} and C_{20} elongase activity in the anadromous teleost meagre (*Argyrosomus regius*). Aquaculture 412–413, 14–22. https://doi.org/10.1016/j.aquaculture.2013.06.032.

Monroig, Ó., Lopes-marques, M., Navarro, J.C., Hontoria, F., 2016. Evolutionary functional elaboration of the Elovl2/5 gene family in chordates. Nat. Publ. Gr. 1–10 https://doi.org/10.1038/srep20510.

Monroig, O., Tocher, D.R., Castro, L.F.C., 2018. Polyunsaturated Fatty Acid Biosynthesis and Metabolism in Fish. Elsevier Inc., Polyunsaturated Fatty Acid Metabolism https://doi.org/10.1016/B978-0-12-811230-4.00003-X.

Morais, S., Monroig, O., Zheng, X., Leaver, M.J., Tocher, D.R., 2009. Highly Unsaturated Fatty Acid Synthesis in Atlantic Salmon : Characterization of ELOVL5- and ELOVL2-like Elongases 627–639. https://doi.org/10.1007/s10126-009-9179-0.

Morais, S., Silva, T., Cordeiro, O., Rodrigues, P., Guy, D.R., Bron, J.E., Taggart, J.B., Bell, J.G., Tocher, D.R., 2012. Effects of genotype and dietary fish oil replacement with vegetable oil on the intestinal transcriptome and proteome of Atlantic salmon (*Salmo salar*). BMC Genomics 13, 448. https://doi.org/10.1186/1471-2164-13-448.

Mourente, G., Bell, J.G., 2006. Partial replacement of dietary fish oil with blends of vegetable oils (rapeseed, linseed and palm oils) in diets for European sea bass (*Dicentrarchus labrax L.*) over a long term growth study: effects on muscle and liver fatty acid composition and effectiveness of a fish oil finishing diet. Comp. Biochem. Physiol. B Biochem. Mol. Biol. 145, 389–399. https://doi.org/10.1016/j.cbpb.2006.08.012.

Oboh, A., Betancor, M.B., Tocher, D.R., Monroig, O., 2016. Biosynthesis of long-chain polyunsaturated fatty acids in the African catfish *Clarias gariepinus*: molecular cloning and functional characterisation of fatty acyl desaturase (fads2) and elongase. Aquaculture 462, 70–79. https://doi.org/10.1016/j.aquaculture.2016.05.018.

Oboh, A., Kabeya, N., Carmona-antoñanzas, G., Castro, L.F.C., Dick, J.R., Tocher, D.R., Monroig, O., 2017. Two Alternative Pathways for Docosahexaenoic Acid (DHA, 22:6n-3) Biosynthesis Are Widespread among Teleost Fish 1–10. https://doi.org/10.1038/s41598-017-04288-2.

Pereira, S.L., Leonard, A.E., Mukerji, P., 2003. Recent advances in the study of fatty acid desaturases from animals and lower eukaryotes. Prostaglandins Leukot. Essent. Fat. Acids 68, 97–106.

Pérez, J.A., Rodríguez, C., Bolaños, A., Cejas, J.R., Lorenzo, A., 2014. Beef tallow as an alternative to fish oil in diets for gilthead sea bream (*Sparus aurata*) juveniles: effects on fish performance, tissue fatty acid composition, health and flesh nutritional value. Eur. J. Lipid Sci. Technol. 116, 571–583. https://doi.org/10.1002/ejlt.201300457.

Reis, D.B., Acosta, N.G., Almansa, E., Garrido, D., Andrade, J.P., Sykes, A.V., Rodríguez, C., 2019. Effect of Artemia inherent fatty acid metabolism on the bioavailability of essential fatty acids for *Octopus vulgaris* paralarvae development. Aquaculture 500, 264–271. https://doi.org/10.1016/j.aquaculture.2018.10.021.

Ribes-Navarro, A., Navarro, J.C., Hontoria, F., Kabeya, N., Standal, I.B., Evjemo, J.O., Monroig, Ó., 2021. Biosynthesis of long-chain polyunsaturated fatty acids in marine gammarids: molecular cloning and functional characterisation of three fatty acyl elongases. Mar. Drugs 19. https://doi.org/10.3390/md19040226.

Rodríguez, C., Pérez, J.A., Henderson, R.J., 2002. The esterification and modification of n-3 and n-6 polyunsaturated fatty acids by hepatocytes and liver microsomes of turbot (*Scophthalmus maximus*). Comp. Biochem. Physiol. Part B Biochem. Mol. Biol. 132, 559–570. https://doi.org/10.1016/S1096-4959(02)00072-6.

Salem, N., Litman, B., Kim, H.Y., Gawrisch, K., 2001. Mechanisms of action of docosahexaenoic acid in the nervous system. Lipids 36, 945–959. https://doi.org/10.1007/s11745-001-0805-6.

Sam, K.-K., Merosha, P., Janaranjani, M., Athirah, I., Shu-Chien, A.C., 2021. The Malaysian Mahseer, *Tor tambroides* possess all required biosynthesis enzymes for the conversion of C18 polyunsaturated fatty acids to long-chain polyunsaturated fatty acids. Aquaculture 543, 736942. https://doi.org/10.1016/j.aquaculture.2021.736942.

Sarker, M.A.-A., Yamamoto, Y., Haga, Y., Sarker, M.S.A., Miwa, M., Yoshizaki, G., Satoh, S., 2011. Influences of low salinity and dietary fatty acids on fatty acid composition and fatty acid desaturase and elongase expression in red sea bream *Pagrus major*. Fish. Sci. 77, 385–396. https://doi.org/10.1007/s12562-011-0342-y.

Sprecher, H., 2000. Metabolism of highly unsaturated n-3 and n-6 fatty acids. Biochim. Biophys. Acta Mol. Cell Biol. Lipids 1486, 219–231. https://doi.org/10.1016/S1388-1981(00)00077-9.

Sprecher, H., Luthria, D.L., Mohammed, B.S., Baykousheva, S.P., 1995. Reevaluation of the pathways for the biosynthesis of polyunsaturated fatty acids. J. Lipid Res. 36, 2471–2477. https://doi.org/10.1016/S0022-2275(20)41084-3.

Tocher, D.R., 1995. Glycerophospholipid metabolism. In: Biochemistry and Molecular Biology of Fishes. Elsevier, pp. 119–157.

Tocher, D.R., 2010. Fatty acid requirements in ontogeny of marine and freshwater fish. Aquac. Res. 41, 717–732. https://doi.org/10.1111/j.1365-2109.2008.02150.x.

Tocher, D.R., Agaba, M., Hastings, N., Teale, A.J., 2003. Biochemical and molecular studies of the polyunsaturated fatty acid desaturation pathway in fish. In: Browman, H.I., Skiftesvik, A.B. (Eds.), The Big Fish Bang - Proceedings of the 26th Annual Larval Fish Conference. Institute of Marine Research, Bergen, Norway, pp. 211–227.

Turchini, G.M., Torstensen, B.E., Ng, W.-K., 2009. Fish oil replacement in finfish nutrition. Rev. Aquac. 1, 10–57. https://doi.org/10.1111/j.1753-5131.2008.01001.x.

Turchini, G.M., Francis, D.S., Du, Z.-Y., Olsen, R.E., Ringø, E., Tocher, D.R., 2022. Chapter 5 - The lipids. In: Fourth, E. (Ed.), Hardy, R.W., Kaushik, S.J.B.T.-F.N. Academic Press, pp. 303–467. https://doi.org/10.1016/B978-0-12-819587-1.00003-3.

Wilson, R., Sargent, J.R., 1992. High-resolution separation of polyunsaturated fatty acids by argentation thin-layer chromatography. J. Chromatogr. A 623, 403–407.

Xie, C., Li, J., Li, D., Shen, Y., Gao, Y., Zhang, Z., 2018. Grass carp: the fish that feeds half of China. In: Gui, J.-F., Tang, Q., Li, Z., Liu, J., De Silva, S.S. (Eds.), Aquaculture in China: Success Stories and Modern Trends. John Wiley & Sons Ltd, pp. 95–115.

Xie, D., Ye, J., Lu, M., Wang, S., You, C., Li, Y., 2020. Comparsion of activities of fatty acyl desaturases and elongases among six teleosts with different feeding and ecological habits. Front. Mar. Sci. 7, 117. https://doi.org/10.3389/fmars.2020.00117.

Xie, D., Chen, C., Dong, Y., You, C., Wang, S., Monroig, Ó., Tocher, D.R., Li, Y., 2021. Regulation of long-chain polyunsaturated fatty acid biosynthesis in teleost fish. Prog. Lipid Res. 82 https://doi.org/10.1016/j.plipres.2021.101095.

Zheng, X., Seiliez, I., Hastings, N., Tocher, D.R., Panserat, S., Dickson, C.A., Bergot, P., Teale, A.J., 2004. Characterization and comparison of fatty acyl Δ6 desaturase cDNAs from freshwater and marine teleost fish species. Comp. Biochem. Physiol. Part B Biochem. Mol. Biol. 139, 269–279. https://doi.org/10.1016/j.cbpc.2004.08.003.